UCID- 21714

ON THE MOVEMENT OF A LIQUID FRONT IN AN UNSATURATED, FRACTURED POROUS MEDIUM, PART I.

John J. Nitao
Thomas A. Buscheck

JUNE 1989

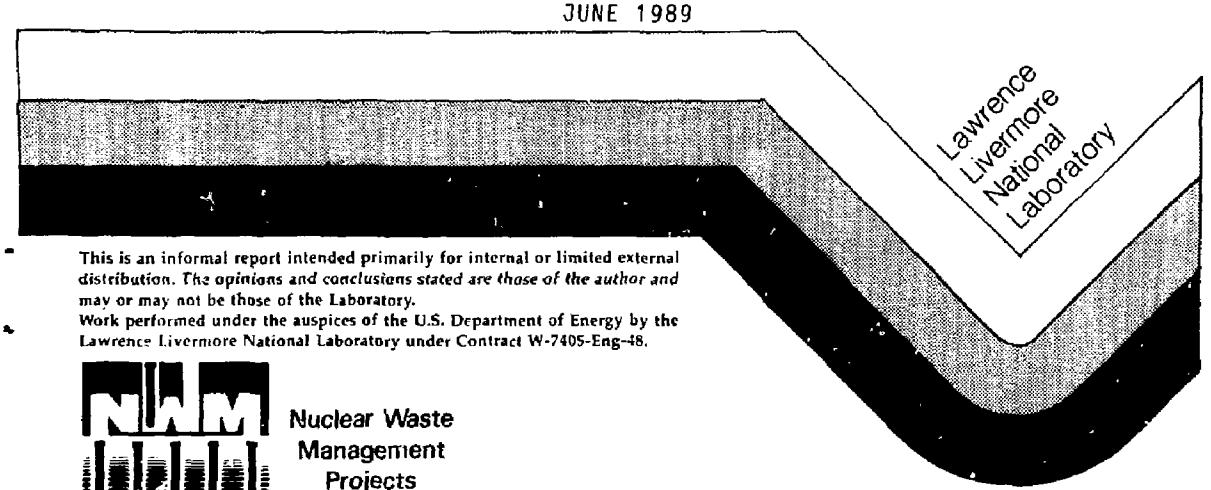

Nuclear Waste
Management
Projects

Prepared by Yucca Mountain Project (YMP) participants as part of the Civilian Radioactive Waste Management Program. The Yucca Mountain Project is managed by the Waste Management Project Office of the U.S. Department of Energy, Nevada Operations Office. Yucca Mountain Project work is sponsored by the DOE Office of Civilian Radioactive Waste Management.

On the Movement of a Liquid Front in an Unsaturated, Fractured Porous Medium, Part I.

John J. Nitao and Thomas A. Buscheck

Earth Sciences Department
Lawrence Livermore National Laboratory

UCID--21714

DE90 006409

ABSTRACT

If a high-level nuclear waste repository is to be built at Yucca Mountain, Nevada, a better understanding of the fracture flow dynamics occurring within unsaturated, fractured rock is needed for its design and licensing. In particular, possible water flow in the rock and fractures will affect waste package design, performance assessment, *in-situ* testing, and site characterization. Most of previous work in fracture flow applies only under saturated hydrological conditions, whereas the Yucca Mountain site is in the unsaturated zone. In this series of papers, as part of the Yucca Mountain Project (YMP), we present an analytical and numerical study of the liquid front movement in a single idealized fracture in an unsaturated porous medium.

The flow of liquid in the fractures is restricted to one dimension and has a property which we have termed *fracture–dominated* flow. This property occurs when the liquid flux in the fracture is sufficiently high that the fracture liquid front advances ahead of the liquid front in the rock. (Sufficient amounts of liquid are assumed to be present at the fracture entrance such that a constant boundary condition is maintained.) Another type of flow, which we call *matrix–dominated*, occurs when the flux into the fracture is low enough that the fracture front lags behind the front in the matrix. These papers will concentrate only on fracture-dominated flow. Matrix-dominated flow will be the subject of future work. We should state here that the issue of when, if, and where these types of flows actually occur at Yucca Mountain has not, at this time, been established and is not the subject of this paper. It is important to note that

fracture-dominated flows will be associated with relatively high fluxes such as when a pond of liquid exists at the fracture entrance.

The primary aim of this paper is to present approximate analytical solutions of the fracture flow which gives the position of the liquid fracture front as a function of time. These solutions demonstrate that the liquid movement in the fracture can be classified into distinctive time periods, or flow regimes. It is also shown that when plotted versus time using a log-log scale, the liquid fracture front position asymptotically approaches a series of line segments. Two-dimensional numerical simulations were run utilizing input data applicable to the densely welded, fractured tuff found at Yucca Mountain in order to confirm these observations.

This work aids understanding of many physical parameters that affect the flow of water in a fractured unsaturated porous medium and, in particular, to some possible hydrological mechanisms occurring at Yucca Mountain. The results could be useful in future analyses requiring the estimation of water movement and in the verification of numerical computer models. Other areas of hydrological study in which our work has direct impact are hazardous waste disposal, petroleum recovery, and flow in soil macropores.

Table of Contents

List of Figures

Nomenclature

Greek Symbols

β	the cosine of the angle of inclination of the fracture from the vertical
χ	$k_r\, d\psi / dS$
λ	fracture storativity ratio, the initial unsaturated pore volume of the matrix relative to the volume of the fracture
Ω	function $\Omega(y)$ denoting the time at which the fracture front first reaches point y
ϕ	matrix porosity
ψ	matrix capillary pressure head
σ	matrix diffusivity, or effective matrix diffusivity
τ	dimensionless time equal to t / t_b
τ_a	t_a / t_b
τ_{bk}	$t_{bk} / t_b, k = 1, 2$
τ^*	dimensionless transition time from boundary dominated flow to flow dominated by gravity and matrix capillary forces

Roman Symbols

a	one-half the distance between adjacent parallel fractures
b	one-half the fracture aperture width
d_{imb}	matrix imbibition penetration depth
h	distance of liquid front leading edge from the fracture entrance
K_f	fracture-saturated hydraulic conductivity
K_m	matrix-saturated hydraulic conductivity
k_r	matrix relative permeability function
L_b	length that the fracture front would travel during time t_b if there were no matrix imbibition
p	pressure in units of liquid head along the fracture
p_c	capillary pressure head at liquid fracture front meniscus
p_0	pressure in units of liquid head at the fracture entrance
$\bar{p}_0$	dimensionless pressure head at the fracture entrance
q	specific volumetric flux into the matrix
q_I	specific imbibition volumetric flux function into the matrix
q_P	specific volumetric flux of water onto to pond located at fracture entrance
q_f	specific volumetric flux at the fracture entrance
Q_m	cumulative specific volumetric flux into the matrix
s	dummy variable of integration
S	liquid saturation in the matrix

S_i initial liquid saturation in the matrix

t time

t_a fracture interference time constant, approximate time for matrix front to reach the no-flow boundary

t_b fracture storativity time constant, approximate time for cumulative matrix imbibition flux to become comparable to the volume in the fracture

u liquid velocity along the fracture

u_0 liquid velocity at the fracture entrance

x coordinate distance normal to the fracture

y coordinate distance longitudinal to the fracture

Z flow region length

1. Introduction

The unsaturated zone at Yucca Mountain, Nevada, is currently being investigated as the possible site for a national high-level nuclear waste repository. The various geological units consist primarily of tuffaceous rock with many of the units being highly fractured [Montazer and Wilson, 1984; Klavetter and Peters, 1986]. The mechanics of water infiltration into unsaturated fractured rock is, therefore, of significant practical importance. In particular, near-field radionuclide transport calculations and waste container design analyses require water influx rates as input parameters. The travel time of water from the waste package to the immediate environment is of primary concern to the overall performance assessment. Characterizing the repository site will require knowing which physical parameters are critical to the flow of water. In turn, this knowledge will depend on the fundamental processes occuring during infiltration into fractured rock. The invasion of drilling water used in construction will be important with regard to the on-site data gathering process in assessing the effects on the *in situ* environment [Buscheck and Nitao, 1988a].

Understanding multiphase fluid processes in fractured porous media is important in other fields of study as well. The secondary recovery of petroleum from naturally fractured reservoirs through water flooding is a prominent example. Our work is also applicable to heterogeneous unsaturated systems where there is a sharp contrast in permeability between two types of materials. For example, the flow in a thin layer of high-permeability rock that is sandwiched between two low-permeability layers is also treatable by our analysis, while another area of study related to our work is the flow of water in soil macropores [Beven and Germann, 1982].

The flow of water in a real-life fractured rock system is complicated by the complex geometry of the fractures and their spatially varying aperture sizes. In general, the path of water may form sinuous channels, or rivulets, of fluid as it flows through a fracture. In the unsaturated zone, further complications arise from the interaction between the fluid in the fractures and the surrounding matrix. Flow restricted to the matrix may possibly occur across fractures by way of contact points [Wang and Narasimhan, 1985]. Before considering these more complicated aspects of fracture flow it would be wise to investigate the simpler problem of flow after the introduction of liquid at one end of a single fracture. We, therefore, consider a single fracture in an initially unsaturated porous medium intersecting a planar exposed face of the rock mass (Figure 1). Suppose that water is allowed to enter into the opening of the fracture with some type of flux or head boundary condition that is uniform across the opening of the fracture. The resulting flow of water in the fracture and the matrix is the focus of this

paper. Note that a sufficient amount of water is assumed to be present at the opening in order to maintain the boundary condition while, at the same time, guaranteeing a continuous front of water. For example, in the case of constant pressure at the opening equal to a value above ambient conditions, a pond of water must exist at the fracture opening.

In some situations the resulting flux into the fracture may be sufficiently low that most of the water will be absorbed through matrix imbibition close to the entrance before any significant fracture flow can occur. Movement of the liquid front, if any, in the fracture will be small and will lag behind the front in the matrix, leading what we have termed in this paper as *matrix–dominated* flow. In other cases, the flux will be sufficiently high that the fracture flow along the longitudinal direction of the fracture will advance ahead of that in the matrix, a situation we will call *fracture–dominated* flow. In this latter case, the speed of the front will be governed by an interaction between the driving forces in the fracture and the suction forces in the matrix. Relatively high fluxes are necessary for this case to occur, such as, if there is ponding of water at the entrance to the fracture. A real fracture system existing in the field will have significant spatial variabilities, and it is possible that these different types of flow conditions may occur simultaneously at different locations in the same fracture. Future work will also have to consider matrix-dominated flows as well as the transition between the two types of flow.

In this series of papers we are interested in fracture-dominated flow. We treat the idealized problem of one-dimensional flow in a uniform aperture, planar fracture. In spite of these simplifications it will be seen that the analysis yields interesting results that may lead, in some cases, to techniques for performing bounding calculations of water movement for more complicated systems as well as an understanding of some fracture flow processes.

In actual field applications the physical parameters that characterize the flow in a fractured system are often difficult to measure and vary significantly in space. Therefore, their values will have a high degree of uncertainty and variance. Thus, from a practical point of view, what can be realistically achieved is to understand the various physical processes present in the system and, it is hoped, to bound the problem. With these goals in mind we have been able, under a class of assumptions, to reduce the governing equations into a single equation of motion describing the movement of the liquid front in the fracture. With this equation we are able to determine the asymptotic behavior of the flow. These solutions are invaluable in revealing various flow processes and flow regimes that may occur and in determining the dependency of the flow on various physical parameters.

Most theoretical work in fracture flow has been restricted to saturated conditions and, until recently, relatively little has been done in unsaturated fracture flow. Travis et al. [1984] have

presented analytic solutions to the problem of a single slug of finite length traveling down a fracture in an unsaturated porous medium with the flux into the matrix assumed to be a constant in time. Numerical solutions were given for more realistic time-varying matrix flux condition. Martinez [1988] has also performed numerical calculations for a continuous front of water and has performed parameter studies applied to Topopah Spring tuff.

We note here that one problem analyzed in this paper is mathematically identical to that considered by J.R. Philip [1968] who looked at the infiltration process in aggregated media. However, most results presented in this paper are believed to be new. Moreover, we are able to show in the context of fracture flow that for the same mathematical problem treated by Philip there exists an "intermediate" flow period in addition to the two periods found by Philip for flow in aggregated media. We also mention here that Davidson [1987] has recently considered infiltration from a saturated fracture of finite length.

Another area where theoretical work in multiphase fracture flow has been active is the secondary recovery of petroleum reservoirs through water flooding. There, workers have been interested in the imbibition of water into a naturally fractured oil-bearing formation. Van Golf-Racht [1982] summarizes the work in this area. Previous analyses in the petroleum literature, however, have not given the detailed behavior of the solutions, nor have they elaborated on the various time constants and length scales important to the front movement process.

2. Assumptions

We consider the flow resulting from the introduction of a liquid into one end of an initially dry planar fracture with constant aperture. The flow inside the fracture is treated as a one-dimensional front with a capillary pressure drop across the leading meniscus. The fracture aperture is assumed to be small enough that, at each point of the fracture front, liquid completely fills the space between the rock walls. The partially saturated rock is assumed to be at uniform initial saturation. In some cases it will be necessary to assume that the matrix diffusivity for capillary imbibition can be approximated by a constant. We will restrict ourselves to the time span of flow until the front reaches the end of the fracture. The fracture is assumed to have no intersections with other fractures.

The arrival of the liquid front in the fracture at any given point on the fracture face will result in a capillary driven flux into the matrix at that point. The flow field in the matrix as a result of these fluxes will, in general, be multi-dimensional. However, if the flow in the system is high enough that it is *fracture-dominated*, as defined earlier, most of the flow lines in the matrix will be primarily orthogonal to the fracture plane (except in the immediate vicinity of the leading edge of the front). Thus, the flow into the matrix at each point on the fracture can be uncoupled and treated individually as that of flow into a one-dimensional sub-system. Because the permeability of the matrix is believed to be many orders of magnitude less than the fractures [Klavetter and Peters, 1986], this treatment is applicable to the various tuffaceous units found at Yucca Mountain. This assumption was also used by Travis et al. [1984] and Martinez [1988], and has been confirmed by our numerical simulations.

Our analysis will not consider the effect of pressure gradients along the length of the fracture upon the imbibition rates into the matrix. This effect will be small if the magnitude of the initial suction pressures in the matrix are large relative to the overpressure in the fracture. We will also assume that the initial suction forces in the matrix are large enough that for the time span of interest the influence of gravity on the matrix flow (but not on the fracture flow) can be neglected.

In applying the solutions covered in this paper one must be careful that the boundary conditions are such that the resulting flow does not violate the above assumptions. In many cases the asymptotic solutions can be used to give guidance concerning whether they are satisfied. Future work will have to be done to derive these conditions and confirm them through numerical simulations. An example of when the boundary conditions may be inappropriate is in the case of a constant flux boundary condition at the fracture opening. If this flux is too low, one may violate the condition of fracture-dominated flow, or the front in the fracture may be stretched by gravity and may separate into more than one piece.

3. The Problem

Matrix Imbibition Flux

We now briefly discuss the form of the imbibition flux into the matrix after passage of the liquid fracture front. The reader is referred to Figure 2 for the coordinate system that is used. Suppose that the matrix has a uniform initial saturation distribution. The equations describing the saturation field in the matrix are

$$\phi \frac{\partial S}{\partial t} = \nabla \cdot K_m k_r \nabla \psi \tag{3.1}$$

$$S(x, y, t=0) = S_i$$

$$S(x=0, y, t) = 1.0 \quad \text{for } y \leq h(t)$$

$$S(x=0, y, t) = S_i \quad \text{for } y > h(t)$$

where

t = time

x = normal distance from fracture

y = longitudinal distance along fracture from fracture entrance

S = liquid saturation

K_m = matrix-saturated hydraulic conductivity

k_r = relative permeability

ψ = capillary pressure head

ϕ = porosity

S_i = initial saturation

$h(t)$ = penetration distance of liquid front in fracture

At a given point y for $y \leq h(t)$ the volumetric flux into the matrix along a single face of the fracture is given by

$$q = -K_m \frac{\partial \psi}{\partial x} \quad \text{at } x = 0 \tag{3.2}$$

In general, this flux depends on location, time, and the past history of the liquid fracture front $h(\tau)$ where $\tau \leq t$, that is,

$$q = q(y, t; h(\tau), \tau \leq t) \tag{3.3}$$

Under the assumptions described in the previous section, the imbibition flux q at a point y on the fracture face will depend only on the time when the front first passes by; that is,

$$q(y,t) = 0 \qquad t \leq \Omega(y) \tag{3.4}$$

$$q(y,t) = q_f(t - \Omega(y)) \qquad t > \Omega(y) \tag{3.5}$$

where $\Omega(y)$ denotes the time when the fracture front first reaches the point y. Here, $q(y,t)$ is the matrix imbibition flux into only one fracture wall.

Fracture Flow

The flow of the liquid in the fracture will be treated as being a front except with a constant capillary pressure drop at the leading meniscus. The one-dimensional fracture is assumed at any given point to be either completely filled with liquid or completely dry. Let $h(t)$ denote the location of the fracture front with respect to the entrance of the fracture. We assume that the liquid in the fracture and matrix is incompressible. Let $u(y,t)$ be the liquid velocity at depth y and time t and let b equal to the constant half-aperture of the fracture. From material balance considerations

$$\frac{\partial u}{\partial y} = -\frac{1}{b} q(y,t) \tag{3.6}$$

Now, let $p(y,t)$ be the liquid phase pressure head in the fracture. Assuming Darcy's law for flow in the fracture, we have

$$u(y,t) = -K_f\left(\frac{\partial p}{\partial y} - \beta\right) \tag{3.7}$$

where K_f is the fracture hydraulic conductivity and β is the cosine of the angle of inclination of the fracture from the vertical. The fracture can be oriented either horizontally or inclined downward relative to its opening. The fracture penetration depth $h(t)$ must satisfy the equation

$$\frac{d\,h(t)}{dt} = u(h(t), t) \tag{3.8}$$

Note that the function $\Omega(y)$ is related to $h(t)$ through the relationship

$$\Omega(h(t)) = t \tag{3.9}$$

and, hence, is the inverse function of $h(t)$.

We will consider two separate types of boundary conditions at the entrance to the fracture: pressure head $p_0(t)$ and flux $u_0(t)$. The pressure head at the leading edge of the front in the fracture is assumed to be at zero datum. Since the equations involve only gradients in head, a non-zero constant

capillary drop $-p_c$ across the leading edge of the front can be included by adding p_c to p_0. We must, however, be careful that the magnitude of the resulting value of p_0 is much smaller than the initial suction pressures in the matrix. Otherwise, significant pressure gradients would occur along the length of the fracture that would couple with the imbibition flux, in violation of one of our basic assumptions. Likewise, the flux boundary condition $u_0(t)$ must not be so large that excessive pressures develop in the matrix. It also must not be so small that it can not meet the the flow demanded by the suction and gravity forces in the fracture; otherwise, the front will become discontinuous violating one of our assumptions. The question of at which critical values of u_0 will these conditions take place will be considered in section 6.4.

Integro-Differential Equations

It can be shown [Nitao, 1989] that the above governing flow equations can, for each of the two types of boundary condition, be reduced to a single integro-differential equation in $h(t)$. These equations are given as

Flux-type boundary condition

$$\frac{dh(t)}{dt} = u_0(t) - \frac{1}{b}\int_0^t q_f(t-s)\frac{dh}{ds}ds \tag{3.10}$$

Pressure-type boundary condition

$$h(t)\frac{dh(t)}{dt} = K_f(h(t)\beta + p_0(t)) - \frac{1}{b}\int_0^t q_f(t-s)h(s)\frac{dh(s)}{ds}ds \tag{3.11}$$

where the solution must satisfy the initial condition

$$h(0) = 0$$

Here, the variable s is a dummy variable of integration.

Fracture Geometry

In this paper we will consider an infinite array of parallel fractures with the same aperture equal to $2b$ (see Figure 3). The spacing between these fractures alternates between distances of $2a_1$ and $2a_2$. The no-flow symmetry lines in the matrix are therefore a_1 from one side of the fracture and a_2 from the other. The matrix blocks can also alternate, not only in their size, but also in their material properties, porosity ϕ_k and diffusivity σ_k $(k = 1, 2)$, as well as initial saturation S_{ik}.

This geometry includes several special cases, such as the case of a single fracture between two semi-infinite matrix blocks ($a_1 = a_2 = \infty$), the case of an infinite array of equally spaced fractures ($a_1 = a_2$), and the case of two parallel fractures with a finite matrix block in between ($a_1 = finite$, $a_2 = \infty$).

In the analysis we will assume constant matrix diffusivities. In [Nitao, 1989] we show that for the case of semi-infinite matrix blocks this assumption is unnecessary and the diffusivity can be a non-constant function of saturation.

4. Flow Periods

Depending on whether we have a constant pressure-type or a constant flux-type boundary condition, we can show that the flow in the fracture undergoes various flow regimes, or time periods, with respect to its interaction with the matrix. During each of these periods the function $h(t)$, which describes the position of the front, can be shown to tend asymptotically toward approximate solutions, which on a log-log scale form a series of line segments giving the general location of the actual solution curve. But first we wish to introduce some relevant time constants and dimensionless groups. As a convention, we will label the two matrix blocks forming the two sides of the fracture as $k = 1$ and $k = 2$. As mentioned, each matrix block can have its own material properties such as porosity ϕ_k and effective diffusivity σ_k. (In the notation of section 3 the diffusivity function is given by $\sigma = (K_m k_r/\phi) d\psi/dS$. Here, we will use the constant "effective diffusivity" defined in Nitao [1989]) The initial saturation S_{ik} can also be different. The fracture spacing a_k was defined in the previous section. From these parameters we define the following relevant time constants

Fracture storativity time constant, t_{bk}

$$t_{bk} = \frac{[2b/(1 - S_{ik})\phi_k]^2 \pi}{\sigma_k} \tag{4.1}$$

Average fracture storativity time constant, t_b

$$\frac{1}{\sqrt{t_b}} = \frac{1}{\sqrt{t_{b1}}} + \frac{1}{\sqrt{t_{b2}}} \tag{4.2}$$

Fracture interference time constant t_{ak}

$$t_{ak} = \frac{a_k^2}{\sigma_k} \pi \tag{4.3}$$

A special case of particular interest is when the fractures are uniformly spaced ($a_1 = a_2$) and the material properties together with the initial saturation of the two matrix blocks are the same. The subscripts in the parameters with respect to the matrix blocks can be dropped. In this case we have

$$t_{bk} = \frac{[2b/(1-S_i)\phi]^2\pi}{\sigma} \tag{4.4}$$

for each block so that from (4.2) one has

$$t_b = \frac{[b/(1-S_i)\phi]^2\pi}{\sigma} \tag{4.5}$$

and from (4.3),

$$t_a = \frac{a^2}{\sigma}\pi \tag{4.6}$$

We are able to show that the solutions can be characterized entirely by the time constants together with the conductivity and fracture orientation. A rigorous derivation is given in [Nitao, 1989], but in this paper we wish to provide some physical motivation behind these time constants. The basis for our discussion follows from the fact that the time t required for a diffusive front to travel a distance L is given approximately by

$$t = \frac{L^2}{\sigma} \tag{4.7}$$

where σ is the diffusivity constant. Since matrix imbibition is primarily a diffusive process, albeit a non-linear one, we expect such a relationship to hold, assuming that we are able to define a characteristic diffusivity constant. Returning to the general case where matrix properties can be different, suppose that imbibition from the fracture is allowed to occur into only one of the matrix blocks. Consider a control volume oriented orthogonal to the fracture (Figure 4) having contact area A with the fracture. Let L be the length of the matrix imbibition front at some given instant of time, and suppose that the saturation along the length of this front is approximately equal to unity. The total volume of the liquid in the front is given by $L\,A\,\phi$ with the portion due to the initial saturation being given by $L\,A\,\phi\,S_i$. Subtracting these two volumes, we obtain that the volume V of liquid absorbed from the fracture by the control volume is given by

$$V = L\,A\,\phi_k\,(1-S_{ik}) \tag{4.8}$$

The portion of the fracture inside the control volume has volume equal to $2b\,A$. When V is equal to this volume we, therefore, have

$$L\,A\,\phi_k\,(1 - S_{ik}) \;=\; 2b\,A$$

$$L \;=\; 2b_k\,/\,\phi_k\,(1 - S_{ik})$$

From (4.7), the time at which these volumes are equal is given by the expression for t_{bk}, except for the factor of π that arises from the rigorous mathematical derivation. Thus, t_{bk} may be interpreted as the approximate time at which the cumulative matrix imbibition from the fracture becomes comparable to the stored volume of the fracture. Although these arguments are heuristic, it is substantiated by rigorous analysis, and gives a useful framework in interpreting the mathematical solutions that will be presented later.

If we now consider imbibition into the two matrix blocks simultaneously, t_b is the approximate time at which the sum of the two cumulative imbibition fluxes leaving the two walls of the fracture is comparable to the specific fracture volume. Note that t_b in (4.5) does not have the factor of two multiplying b that is present in t_{bk} since each of the two matrix blocks share one half of the fracture volume. The other time constants t_{a_k} are simply the approximate times at which the imbibition front in matrix k reaches the no-flow symmetry line with the respective neighboring fracture. It is interesting to note that although the definition of the time constants assumes a constant or almost constant matrix diffusivity, their physical definitions remain valid even when the diffusivity is a function of saturation, and are, therefore, applicable even when this assumption does not hold.

We define the following ratios:

Matrix–to–fracture storativity ratio, λ_k

$$\lambda_k \;=\; \sqrt{\frac{t_{ak}}{t_{bk}}} \;=\; \frac{a_k\,(1 \;-\; S_{ik})\,\phi_k}{2b} \tag{4.9}$$

Total storativity ratio, λ

$$\lambda \;=\; \lambda_1 \;+\; \lambda_2 \tag{4.10}$$

The dimensionless constants λ_k are the ratios of the initial unsaturated pore volume of the kth matrix to the volume of the fracture while λ is the ratio of the total initial pore volume in the matrix to the fracture. When the fractures are spaced uniformly and the matrix properties are the same, we have from (4.9) and (4.10) that λ reduces to

$$\lambda \;=\; \sqrt{\frac{t_a}{t_b}} \;=\; \frac{a\,(1 \;-\; S_i)\,\phi}{b} \tag{4.11}$$

In order to simplify the discussion, suppose that the matrix blocks on both sides of the fracture have the same flow properties and that we have a system of parallel fractures with equal spacing. With this assumption we have $t_a = t_{a1} = t_{a2}$. Analyses presented in Nitao [1989] show that with constant-time boundary conditions, there will generally be three major time periods for the movement of the liquid fracture front. These time periods can be shown to arise from the three stages of matrix imbibition that can occur at any given point on the fracture face. Let us focus our attention on a single slice of infinitesimal thickness that is orthogonal to the fracture (Figure 5). Suppose that the fracture front has just reached this slice, and imbibition begins. Stage A for this slice occurs when the cumulative volume of liquid that has imbibed is less than the fracture volume inside the slice. Stage B is when the imbibed volume in the matrix has increased to an amount greater than the fracture volume, but before the matrix front reaches the no-flow symmetry boundary of the matrix block due to neighboring fractures. Stage C occurs after the front reaches the matrix no-flow boundary. The matrix can, therefore, be divided into three zones depending on the stage of imbibition (Figures 6 and 7) with zone I corresponding to those points that lie on slices undergoing stage A, zone II corresponds to stage B, and zone III to stage C. These zones propagate with the liquid front as it proceeds into the fracture with zone I occuring near the tip of the fracture liquid front, followed by zone II, and, then, by zone III.

Which time period is occuring depends on which of the zones is the largest. At early times, $t \leq t_b$, most or all of the fracture front lies in zone I, and the flow in the fracture is, therefore, influenced only weakly by matrix imbibition and is, instead, dominated by the fracture boundary condition and gravity. As the fracture front proceeds, a significant part of the matrix is in zone II, i.e. cumulative imbibition fluxes are comparable to the fracture volume, and the front is slows down. During this second flow period, $t_b \leq t \leq t_{a1}$, there is a balance between (1) matrix suction forces and (2) gravity and, possibly, (3) fracture flow boundary conditions. Finally, as the matrix imbibition front approaches the no-flow symmetry planes, the imbibition flux begins to decline, and we enter the third flow period, $t_a \leq t$ when most of the matrix is in zone III.

We are also able to treat other cases: when the matrix blocks do not have the same material and initial properties, and when the fractures are not evenly spaced. In general, we then have $t_{a1} \neq t_{a2}$. (In the rest of the paper we can assume, without loss of generality, that $t_{a2} \geq t_{a1}$. Otherwise, the indices 1 and 2 are interchanged in what follows.) The only difference from the equal fracture spacing case is that the third flow period is split into two sub-periods IIIa and IIIb because matrix $k = 1$ enters flow period III while matrix $k = 2$ is still in period II. In particular, there is a period $t_{a1} \leq t \leq t_{a2}$ corresponding to when only matrix block $k = 1$ is in flow period III. For later times, $t_{a2} \leq t$, matrix block $k = 2$ is also in flow period III. (These flow periods apply if

$t_b \leq t_{a1} \leq t_{a2}$, which will be true in most cases. Other less likely orderings of the time constants will lead to other flow periods.)

To summarize, the flow periods are:

Flow period I (boundary and gravity dominated)

$$t \leq t_b \tag{4.12}$$

Flow period II. (balanced)

$$t_b \leq t \leq t_{a1} \tag{4.13}$$

Flow period IIIa (reduced matrix suction in a single matrix block)

$$t_{a1} \leq t \leq t_{a2} \tag{4.14}$$

Flow period IIIb (reduced matrix suction in both matrix blocks)

$$t_{a2} \leq t \tag{4.15}$$

If a flow period has upper and lower time limits that are comparable or if the upper becomes less than the lower, that particular flow period will not be present. For example, when t_b is comparable to, or greater than t_{a1}, flow period II is non-existent.

In some situations, special degenerate cases can occur depending on how the time constants are ordered. For example, suppose that one of the matrix blocks bounding the fracture is much larger than the other but with their diffusivities being equal. That is, $a_2 >> a_1$ and $\sigma_1 = \sigma_2$. It can then be seen that $t_{a1} << t_{a2}$. Moreover, suppose that the initial unsaturated pore volume of matrix block $k = 1$ is much smaller than the fracture pore volume, which in turn is much smaller than the initial unsaturated pore volume of matrix block $k = 2$. We then have the situation where $t_{a1} << t_b << t_{a2}$. While in flow period II the total imbibition flux into block $k = 1$ will start to decline relatively early because of the small matrix volume of this block and and will then go into flow period III. This transition will happen before the flux into block $k = 2$ has become significant enough to go into flow period II. The flow in the fracture will revert to being *boundary- or gravity-dominated*, and instead of *Flow period IIIa* we have two periods which we call *IIIa.1* and *IIIa.2*.

Flow period IIIa.1 (revert to boundary or gravity dominated)

$$t_{a1} \leq t \leq t_{b2} \tag{4.16}$$

Flow period IIIa.2 (partially reduced suction)

$$t_{b2} \leq t_{a2} \tag{4.17}$$

In order for this situation to occur we must have $t_{a1} \leq t_{b2} \leq t_{a2}$. It is obvious that there are other orderings of the time constants that can lead to special flow periods not covered by those given here. However, in most situations, such as when both matrix sides of the fracture have nearly identical matrix properties and initial saturations, the three periods we have given in (4.12) to (4.15) are the only major ones. The other subcases can be treated, if desired, by using the techniques in Nitao [1989].

5. Dimensionless Groups

It will be seen later that a convenient definition of dimensionless time is obtained by taking time to be relative to the time constant t_b. Therefore, let us denote by τ the dimensionless time given by

$$\tau = t / t_b \tag{5.1}$$

It will also be convenient to normalize the other time constants relative to t_b:

$$\tau_{ak} = t_{ak} / t_b \tag{5.2}$$

$$\tau_{bk} = t_{bk} / t_b \tag{5.3}$$

The index $k = 1, 2$ refers to the matrix blocks bounding the fracture. In terms of normalized time the flow periods are given as follows.

Flow period I (fracture flow boundary and gravity dominated)

$$\tau \leq 1 \tag{5.4}$$

Flow period II (balanced)

$$\tau_b \leq \tau \leq \tau_{a1} \tag{5.5}$$

Flow period IIIa (reduced matrix suction in a single matrix block)

$$\tau_{a1} \leq \tau \leq \tau_{a2} \tag{5.6}$$

Flow period IIIb (reduced matrix suction in both matrix blocks)

$$\tau_{a2} \leq \tau \tag{5.7}$$

The fracture penetration length, h, can be made dimensionless $\bar{h}$ by dividing by L_b, which is defined to be the distance that would be traveled by the fracture front at time $t = t_b$ if no imbibition

into the matrix were present. These "imbibition-free" length scales L_b can be easily derived for the various combination of boundary conditions and are given in Table I. For example, in the case of $p_0 = 0$ with gravity, liquid will travel down the fracture flow at a constant speed equal to $K_f \beta$. Thus, at time t_b it will have traveled a distance equal to $L_b = K_f \beta t_b$. To understand further the meaning of L_b, note that the gravity and boundary pressure forces including fracture capillarity will dominate over matrix imbibition when the fracture penetration is less than L_b since the imbibition into the matrix is relatively unimportant for $t < t_b$. In Table I, the last row corresponds to a pressure boundary condition with gravity. There, the value of the length scale L_b is computed based on the value computed due to gravity and with the boundary pressure p_0 set to zero.

Table I Fracture Penetration Length Scale L_b

Boundary Condition	L_b
flux b.c.	$u_0 t_b$
pressure b.c no gravity	$\sqrt{2 K_f p_0 t_b}$
pressure b.c with gravity	$K_f \beta t_b$

In some cases we will also need to define a dimensionless boundary pressure head obtained by normalizing with respect to $K_f \beta^2 t_b$

$$\bar{p}_0 = p_0 / K_f \beta^2 t_b \tag{5.8}$$

Note that the normalization of $\bar{p}_0$ has a factor of β^2 instead of the single factor of β that is present in the normalization of h given above. Without going into a detailed mathematical analysis at this point, it suffices to say that a natural normalization of the pressure head is with respect to the gravity head βh of the liquid column in the fracture. In order to make h dimensionless, this expression can be rewritten as $\beta L_b \bar{h} = K_f \beta^2 t_b \bar{h}$, which has the factor of β^2, in addition to the other factors, in (5.8). We would also like to point out, here, that any capillary head drop $-p_c$ across the leading edge of the fracture front can be included into p_0 by adding p_c; thus, the dimensionless pressure includes the dimensionless fracture capillary pressure.

6. Asymptotic Behavior

6.1 Penetration Depth

The asymptotic solutions to (3.10) and (3.11) are derived in Nitao [1989] for the cases where the $u_0(t)$ or p_0 boundary conditions are constant in time. The solutions for flow periods I and II holds for general diffusivity functions, while in the mathematical analysis for flow period III it was necessary to assume that the matrix diffusivity is approximately constant. In developing a solution for the pressure boundary case, (3.11), it was convenient for the purposes of exposition to split the problem into (1) the case without gravity (i.e., $\beta = 0$) and (2) the case with gravity. At early time for the latter case, one must also distinguish whether p_0 is zero or non-zero relative to ambient head.

In Table II we have summarized the leading terms of the asymptotic expansion for the dimensionless fracture penetration depth $\bar{h}$ for the different types of boundary conditions and for the different flow regimes. The dimensionless variables used here are described in the previous section. The higher order terms are derived and presented in Nitao [1989]. Note that all expansions are powers of the dimensionless time τ. When the value of the upper limit of a time period is less than the lower, that particular flow period is not present (e.g., if $\tau_{a1} < 1$, then flow period II is not observed, and if $\tau_{a2} \leq \tau_{a1}$, then IIIa is not).

The expansions in column 2 of Table II for the pressure boundary condition case with no gravity (i.e., $\beta = 0$) is a special case of the general expansion given in column 4 and corresponds to the case of a horizontal fracture. Note that during flow period II, for this particular case, the fracture penetration goes as the one-quarter power in time, which is slower than the one-half power movement of the matrix saturation front in the direction longitudinal to the fracture. Hence, the matrix front will eventually overtake the fracture front unless flow period III, with its faster one-half power behavior begins sufficiently early. In his theoretical study of aggregated soils Philip [1968] derived asymptotic solutions equivalent to those in flow periods I and III (column 2 of Table II) but he did not consider the intermediate flow period II, probably because this period is not of significant duration for aggregated soils which, because of their relatively small granules, have corresponding time constants with t_b comparable to t_a.

The fixed pressure boundary condition with $p_0 = 0$ given in column 3 of Table II pertains to the case when the pressure head at the fracture entrance is held at ambient. It is a special case of the solution given in column 4, which includes the general boundary condition in pressure. We have included

Table II. Leading Term of Expansion for Dimensionless Penetration $\bar{h}$

	1	2	3	4
flow period (range of high accuracy)	flux $\bar{h} = \frac{h}{u_0 t_b}$	pressure b.c no gravity $\bar{h} = \frac{h}{\sqrt{2p_0 K_f t_b}}$	pressure b.c $p_0 = 0$, gravity $\bar{h} = \frac{h}{K_f \beta t_b}$	pressure b.c $p_0 \neq 0$, gravity $\bar{h} = \frac{h}{K_f \beta t_b}$
I ($\tau << 1$)	τ	$\tau^{1/2}$	τ	$\tau^{1/2}\sqrt{2\bar{p}_0}$, $\tau << \bar{p}_0$ $\frac{2}{3}\tau$, $\tau >> \bar{p}_0 > 0$ τ, $\bar{p}_0 = 0$
II ($1 << \tau << \tau_{a1}$)	$\frac{2}{\pi}\tau^{1/2}$	$\sqrt{\frac{2}{\pi}}\tau^{1/4}$	$\tau^{1/2}$	$2\sqrt{\frac{\bar{p}_0}{\pi}}\tau^{1/4}$, $\tau << \bar{p}_0^{\,2}$ $\tau^{1/2} + \frac{(2\bar{p}_0 - 1)}{(\pi - 2)}$, $\tau >> \bar{p}_0^{\,2}$
IIIa ($\tau_{a1} << \tau << \tau_{a2}$)	$\frac{2}{\pi}(\tau_{b2}\tau)^{1/2}$	$\sqrt{\frac{2}{\pi}}(\tau_{b2}\tau)^{1/4}$	$(\tau_{b2}\tau)^{1/2}$	$2\sqrt{\frac{\bar{p}_0}{\pi}}(\tau_{b2}\tau)^{1/4}$, $\tau << \bar{p}_0^{\,2}/\tau_{b2}$ $(\tau_{b2}\tau)^{1/2} + \frac{(2\bar{p}_0 - \tau_{b2})}{(\pi - 2)}$, $\tau >> \bar{p}_0^{\,2}/\tau_{b2}$
IIIb ($\tau_{a2} << \tau$)	$\frac{1}{1+\lambda}\tau$	$\frac{1}{\sqrt{1+\lambda}}\tau^{1/2}$	$\frac{1}{1+\lambda}\tau$	$\sqrt{\frac{2\bar{p}_0}{1+\lambda}}\tau^{1/2}$, $\tau << \bar{p}_0(1+\lambda)$ $\frac{1}{1+\lambda}[\tau + A\tau^{1/2}]$, $\tau >> \bar{p}_0(1+\lambda)$ $A = \left[\frac{2}{3}\frac{\lambda_1\tau_{a1} + \lambda_2\tau_{a2}}{1+\lambda} + 2\bar{p}_0(1+\lambda)\right]^{1/2}$

column 3 in the table because of its simplicity relative to the more general case in column 4. The situation is complicated in column 4 by the interplay between gravity and the pressure boundary condition. For each of the flow periods in column 4 there are two possible expansions, one pertaining to the time period during which the boundary pressure dominates fracture flow and one for when gravity and matrix imbibition dominates; the applicable expansion is determined by the relationship of the dimensionless transition time τ^* and the limits of the respective flow period. If τ^* is less than the lower limit, the second expansion applies over the entire interval. If τ^* is greater than the upper limit, the first expansion is applicable, and if τ^* is between the limits, the first expansion applies for $\tau \leq \tau^*$ and the second for $\tau \geq \tau^*$. The value of τ^* depends on the flow period and is a function of the dimensionless boundary pressure head $\bar{p}_0$,and the matrix-fracture storativity ratio λ. From Table II we see that it is equal to $\bar{p}_0$, $\bar{p}_0^{\,2}$, $\bar{p}_0^{\,2}/\tau_{b2}$, $\bar{p}_0\lambda$ for flow periods I, II, IIIa, and IIIb, respectively. With one exception, the value of τ^* for a given $\bar{p}_0$ and λ can be shown to lie in only one of the flow periods, and, hence, the transition occurs only once. The exception is if $\tau_{a2} < \bar{p}_0 < \sqrt{\tau_{a2}\tau_{b2}}$; in which case, the transition time is in both flow periods IIIa and IIIb. Thus, in period IIIa there can be a transition from

boundary dominated to matric capillary-gravity, and, then, reversion to boundary dominated at the beginning of period IIIb, and, finally, a return to matric capillary-gravity dominated flow.

As we mentioned earlier, if $t_{a1} << t_{b2} << t_{a2}$, then flow period IIIa is replaced by IIIa.1 and IIIa.2. The expansions for these two subperiods are given in Table III.

Table III. Leading Term of Expansion for Dimensionless Penetration $\bar{h}$ (special subcase)

	1	2	3	4
flow period (range of high accuracy)	pressure b.c. $p_0 \neq 0$, gravity $\bar{h} = \frac{h}{K_f \beta r_b}$			
IIIa.1 $(\tau_{a1} << \tau << \tau_{b2})$	$\frac{1}{1+\lambda_1}\tau$	$\frac{1}{\sqrt{1+\lambda_1}}\tau^{1/2}$	$\frac{1}{1+\lambda_1}\tau$	$\frac{1}{1+\lambda_1}\left[\tau + (\tau_{b1}\tau)^{1/2}\left\{\frac{2}{3}\frac{\lambda_1^{3/2}}{1+\lambda_1} + 2\bar{p}_0(1+\lambda_1)\right\}^{1/2}\right]$
IIIa.2 $(\tau_{b2} << \tau << \tau_{a2})$	same as for period IIIa of Table II	same as for period IIIa of Table II	same as for period IIIa of Table II	same as for period IIIa of Table II

The special case, $\tau_{a_1} = \tau_{a_2}$ and $\tau_{b_1} = \tau_{b_2}$, is of interest because of its relative mathematical simplicity, and since it includes the equal fracture spacing case with the matrix blocks having the identical properties. The expressions in column four of Table II can be reduced to this case by first removing flow period IIIa, changing flow period IIIb to III, and making the following substitutions: $\lambda_1 = \lambda_2 = \lambda/2$, $\tau_{a1} = \tau_{a2} = \tau_a$. Table IV shows the dimensionless fracture penetration for this case with gravity and non-zero boundary pressure condition. As will be shown later, the dimensionless transition time τ^* from boundary to matric capillary-gravity dominated flow lies in only one of the time periods, and, therefore, the transition occurs only once.

Table IV. Leading Term of Expansion for Dimensionless Penetration $\tilde{h}$ when $\tau_{a_1} = \tau_{a_2}$ and $\tau_{b_1} = \tau_{b_2}$

flow period (range of high accuracy)	pressure b.c. $p_0 \neq 0$, gravity $\tilde{h} = \dfrac{h}{K_f \beta L_b}$
I ($\tau << 1$)	$\tau^{1/2}\sqrt{2\bar{p}_0}$, $\tau << \bar{p}_0$ $\dfrac{2}{3}\tau$, $\tau >> \bar{p}_0$ τ, $\bar{p}_0 = 0$
II ($1 << \tau << \tau_{a_2}$)	$2\sqrt{\dfrac{\bar{p}_0}{\pi}}\tau^{1/4}$, $\tau << \bar{p}_0^{\,2}$ $\tau^{1/2} + \dfrac{(2\bar{p}_0 - 1)}{(\pi - 2)}$, $\tau >> \bar{p}_0^{\,2}$
III ($\tau_{a_2} << \tau$)	$\sqrt{\dfrac{2\bar{p}_0}{1+\lambda}}\tau^{1/2}$, $\tau << \bar{p}_0(1+\lambda)$ $\dfrac{1}{1+\lambda}[\tau + A\tau^{1/2}]$, $\tau >> \bar{p}_0(1+\lambda)$ $A = \left[\dfrac{2}{3}\dfrac{\lambda^{3/2}}{1+\lambda} + 2\bar{p}_0(1+\lambda)\right]^{1/2}$

6.2 Effects of Fracture Capillarity

We saw earlier that the boundary condition p_0 can include the capillary pressure across the leading meniscus of the fracture front by adding the magnitude of the capillary head p_c to the entrance pressure. Let us consider the case where the fracture entrance is kept at ambient pressure so that p_0 is equal to p_c. For a vertical fracture system ($\beta = 0$), we ask the question: When is fracture capillarity the dominant driving force ? Let us assume that the fractures have equal spacing and identical matrix properties so that the results of Table IV hold. From that table the transition time τ^* from boundary dominated (in this case fracture capillary pressure) to matric capillary-gravity dominated flow is seen to occur in flow period I if $p_c / L_b << 1$, flow period II if $1 << p_c / L_b << \lambda$, and flow period III if $\lambda << p_c / L_b$. Here, we used the fact that $\tau_a = \lambda^2$ and $\bar{p}_0 = p_0 / L_b$. Note that these three conditions on p_c are mutually exclusive so that the transition occurs at a single point in time and no reversion to fracture capillary dominated flow occurs once it starts. It is also interesting to note that the fracture penetration h at time $\tau = \tau^*$ can be shown to be approximately equal to p_c. Thus, the transition out of the fracture capillarity regime occurs when the hydrostatic head of the liquid in the fracture

becomes comparable to the fracture capillary head.

6.3 Fracture Influx Rate

The specific volumetric influx rate q_f is defined to be the flux per fracture flow area into the entrance to the fracture, and hence, is equal to the liquid velocity into the fracture. The first-order asymptotic expansions for the influx rate are given in Table V for the constant pressure boundary value problem, with and without gravity.

Table V. Leading Term of Expansion for Fracture Inflow Velocity, Pressure B.C.'s

flow period	no gravity $\frac{q_f}{\sqrt{2K_f p_0 / t_b}}$	gravity, $p_0 = 0$ $\frac{q_f}{K_f \beta}$
I	$\frac{1}{2}\tau^{-1/2}$	$\sqrt{\frac{\tilde{p}_0}{2}}\,\tau^{-1/2}$, $\tau << \tilde{p}_0$ 1.0, $\tau >> \tilde{p}_0$
II	$\sqrt{2}\frac{\Gamma(5/4)}{\Gamma(3/4)}\tau^{-1/4}$	$\frac{1}{2}\frac{\Gamma(1/4)}{\Gamma(3/4)}\sqrt{\tilde{p}_0}\,\tau^{-1/4}$, $\tau << \tilde{p}_0^{\,2}$ $\frac{\pi}{2}$, $\tau >> \tilde{p}_0^{\,2}$
IIIa	$\sqrt{2}\frac{\Gamma(5/4)}{\Gamma(3/4)}(\tau_{b2}\tau)^{-1/4}$	$\frac{1}{2}\frac{\Gamma(1/4)}{\Gamma(3/4)}\sqrt{\tilde{p}_0}\,(\tau_{b2}\tau)^{-1/4}$, $\tau << \tilde{p}_0^{\,2}/\tau_{b2}$ $\frac{\pi}{2}$, $\tau >> \tilde{p}_0^{\,2}/\tau_{b2}$
IIIb	$\frac{1}{2}\sqrt{1+\lambda}\,\tau^{-1/2}$	$(1+\lambda)\sqrt{\frac{\tilde{p}_0}{2(1+\lambda)}}\,\tau^{-1/2}$, $\tau << \tilde{p}_0(1+\lambda)$ 1.0, $\tau >> \tilde{p}_0(1+\lambda)$

These expressions were obtained by applying Laplace transform techniques [Nitao, 1989]. Note that the flux decays as a power of time for the no-gravity case. The gravity case decays in a similar fashion until the transition time τ^* is reached. For times greater than τ^* the specific influx rate for the gravity case becomes, to the first order, approximately a constant in time, varying within the relatively narrow range of $K_f\,\beta$ to $\pi K_f\,\beta/2$. Influx rates determined by the numerical solutions to the integro-differential equation with no capillarity confirm this fact (see Figure 8). This observation is also corroborated by the fact that when we substitute the expression for q_f from Table V, column 2, for u_0 in

Table II, column 1, we obtain the same leading order term for h as in Table II, column 3.

Note that the influx rate for the no-gravity case varies with respect to time as $t^{-1/2}$ for early and late times, as in a typical imbibition process for homogeneous media. But, for intermediate times a higher rate $t^{-1/4}$ is seen to occur, unlike homogeneous media. Upon integrating these expressions with respect to time, the cumulative imbibition flux into a highly fractured horizontally oriented core with longitudinal fractures varies as $t^{1/2}$ at early and late times but has an intermediate period where the cumulative flux picks up and goes approximately as $t^{3/4}$. A qualitatively similar effect is expected to occur for a heterogeneous porous media with two highly separated modal distribution of pore sizes. Although for early or late times the imbibing fractured medium can be considered to behave as a single effective homogeneous porous medium, we see that during the intermediate flow period this conclusion is not valid.

6.4 Front Continuity and the Drainage Capacity of Fractures

We now apply the results of the previous subsection to the question of front continuity and drainage capacity for a pond, or pool, of water drained by a fracture. Suppose that the pond is charged solely by a constant volumetric flux q_P of water (this flux as many of those in this paper are specific fluxes relative to the transverse width of the fracture). Gravity is present, and we assume that initial depth of the pond is negligible so that the resulting hydrostatic head at the fracture entrance is approximately zero relative to ambient. We restrict ourselves here to sufficiently late times when fracture capillarity is not important.

If the pond is of finite extent, the flux into the pond must equal that which drains into the fracture, i.e., $q_P = 2b\, q_f$, in order that a constant level is maintained. As before, q_f is the specific flux into the fracture. Obviously, if the flux into the pond exceeds the fracture flux, the pond will rise while if the flux is less, the pond will sink, and the front of water will no longer be continuous from the fracture entrance to the leading front. Since Figure 8 gives the fracture flux, we can deduce when these events occur. If $q_P / 2b\, K_f \beta \leq 1$, we must have $q_f / K_f \beta \leq 1$ in order to maintain a constant pond level. But, since the fracture flux is seen in Figure 8 to always lie above this value the pond level will decrease, and the fracture liquid front will separate. Under these conditions the fracture is able to drain the pond. If $q_P / 2b\, K_f \beta \geq \pi/2$, we have $q_f / K_f \beta \geq \pi/2$. From Figure 8, the fracture flux always lies below this value so that the pond level will rise, and the fracture is not able to drain the pond. In

between these two flux values, the pond will drain for early and late times but will rise at intermediate times.

6.5 Matrix Flow Regions

In section 4 we showed that matrix saturation field can be classified by depth into various zones, or flow regions, based on the flow periods. In general, the division of the two matrix blocks into zones will be different on each side of the fracture. For simplicity, consider the situation where the matrix blocks have similar properties so that their zones are the same. Table VI lists asymptotic approximations of the lengths of zones I and II which were derived for times $t >> 2t_a$, based on the asymptotic expansions of Table II. They are made dimensionless through dividing by L_b which would be the fracture penetration distance at time t_b if no matrix imbibition occurred. Note that for the influx boundary condition and gravity-driven cases (columns 1 and 3 in Table VI) the dimensionless length of zone II approaches a constant equal to $\lambda - 1$ at infinite time. Hence, in the limit, the matrix imbibition front lags behind the fracture front by a fixed amount. Several theoretical and experimental investigations have reported this result [Bokserman, et al., 1964; Marle, 1981]. To our knowledge, this paper is the first to mathematically derive an expression for this length. Recall that λ is the ratio of the initial unsaturated pore volume in the matrix to the fracture. In many cases this ratio will be much greater than one, and therefore, $\lambda - 1 \approx \lambda$. Hence, in such cases, the dimensionless distance that the matrix lags the fracture front is equal to the ratio of the initial pore volume in the matrix to the fracture volume, which is the same value for the lag length as given in the above references.

For the pressure boundary condition with no gravity (column 2), the lengths of zones I and II approach zero at infinite time. Hence, in the limit, the matrix front catches up with the fracture front. The disappearance of zones I and II is indicative of equilibrium being attained between the fracture and matrix saturation fields along the entire wetted interval of the fracture.

Table VI. Expansions for Flow Region Lengths, $\tau >> 2\tau_a$, $\lambda \geq 1$

	1	2	3
dimensionless length	flux b.c.	pressure b.c no gravity	pressure b.c gravity, $p_0 = 0$
Z_1/L_b	$1/(1+\lambda)$	$\frac{1}{2}\frac{1}{\sqrt{1+\lambda}}\tau^{-1/2}$	$1/(1+\lambda)$
Z_2/L_b	$\lambda - 1$	$\frac{1}{2}\frac{\lambda^2-1}{\sqrt{1+\lambda}}\tau^{1/2}$	$\lambda - 1$

7. Asymptotic Fracture Penetration Profiles

It is an interesting fact that the first-order terms of all of the asymptotic expansions are powers in time $\bar{h} \sim \tau^m$ and, when plotted on a log-log scale, will form a series of straight line segments with a corresponding slope m for each flow period. In Figures 9 to 13 we have drawn the generic "penetration profiles" for the three types of boundary conditions that were considered. The line segments are labeled with their respective slopes. For simplicity, we have restricted ourselves in these diagrams to the case when the fracture spacings are equal. Note that in figures 9 and 10 there is a single family of dimensionless curves parameterized with respect to λ. For figures 11 to 13 the curves are characterized by λ and $\bar{p}_0$. Recall that the parameter $\bar{p}_0$ is the ratio of the drop in pressure head across the front (due to boundary head at the entrance and the capillary head at the meniscus) to βL_b (also recall that $L_b = K_f \beta t_b$). Figure 11 corresponds to the case when $\bar{p}_0 < 1$. The first line segment on the left corresponds to the flow period during which the pressure drop is small relative to the hydrostatic head. For the case in Figure 12 when $1 \leq \bar{p}_0 \leq \lambda$, the pressure drop is larger than the imbibition-free head so that the the boundary pressure dominated regime extends past $\tau = 1$ into the time period II, $1 \leq \tau \leq \tau_a$. Figure 13 corresponds to the case where $\lambda \leq \bar{p}_0$ and is boundary pressure dominated until $\tau^* = \bar{p}_0 \lambda$ in period III, $\tau_a \leq \tau$.

These plots have the potential to become useful calculational tools, and are particularly helpful in visualizing the dependence of the asymptotic solutions on the various parameters.

8. Parameter Variation

We now consider the effect of parameter variation on the fracture penetration for a particular geometry. Consider a vertical fracture with the boundary pressure at the entrance kept at ambient conditions. Such a boundary condition would occur if a shallow pond was present at the entrance. Because of the vertical orientation, gravity is present. The initial saturation and material properties of the two matrix blocks bounding the fracture are assumed to be identical. The expressions for the fracture penetration h are listed in Table VII and are dimensional in order to illustrate the dependence on the various system parameters. It is important to note that this table assumes that we stay within a

single flow period as the parameters are varied. In some cases, because of large parameter changes, we may switch into a different flow period. Although these expressions are based on first-order asymptotic approximations, comparisons with numerical calculations indicate that they adequately represent the proper parameter sensitivities. We have assumed that the diffusivity σ can be approximated as a constant. In order to separate the dependence of the diffusivity on the porosity and conductivity, we write

$$\sigma = K_m \chi / \phi$$

The constant χ is defined here to be some averaged value of $k_r \, d\psi / dS$ where k_r is the relative conductivity and ψ is the capillary head as a function of saturation. The time constants can be written as

$$t_b = \frac{4\pi b^2}{(1-S_i)^2 \phi K_m \chi} \tag{8.1}$$

$$t_a = \frac{\pi a^2 \phi}{K_m \chi} \tag{8.2}$$

Table VII. Dependence of Fracture Penetration on Parameters ($p_0 = 0$, equal matrix properties)

Flow Period I. $0 \le t \le t_b$	$h \sim K_f t$	
Flow Period II. $t_b \le t \le t_a$	$h \sim \frac{K_f b}{1-S_i} \sqrt{\frac{\pi}{\phi K_m \chi}} \, t^{1/2}$	
Flow Period III. $t_a \le t$	$h \sim \frac{K_f}{1 + a\phi(1-S_i)/b} t$	
	$h \sim \frac{K_f b}{a\phi(1-S_i)} t$	if $a\phi(1-S_i) >> b$
	$h \sim K_f t$	if $a\phi(1-S_i) << b$

In Table VII we see that h depends linearly on K_f for all times. We also see that the h versus K_m dependence is significant only during flow period II. However, from (8.1) and (8.2), we see that the time constants which define the ranges in the flow periods, t_a and t_b vary as K_m^{-1}. During flow period I the fracture penetration h is insensitive to the matrix porosity ϕ while it varies as $\phi^{-1/2}$ during period II. During period III, if $a\phi(1-S_i) >> b$, the sensitivity to ϕ becomes even more pronounced, with h varying as ϕ^{-1}. Regarding the initial matrix saturation S_i, if we neglect the dependence of χ on S_i, we have that h varies as $(1-S_i)^{-1}$ during flow periods II and III while it is insensitive to S_i during flow period I. As expected, only during flow period III is h sensitive to the fracture spacing a. However, the time constant t_a is very sensitive to a, varying as a^2. In order to elucidate the dependence of h on the fracture half aperture b, let us suppose that the saturated fracture hydraulic conductivity K_f varies

as b^2 in accordance with some form of the widely used "cubic law" as given by Pouiselle flow theory (see, for example, Huyacorn and Pinder [1983]). Thus, the fracture penetration h varies as b^2 during flow period I and as b^3 during period II. During period III the fracture penetration h varies as b^2 if $a\phi(1-S_i) << b$ and as b^3 if $a\phi(1-S_i) >> b$. It is, perhaps, not surprising that h is most strongly affected by the fracture aperture b. Note that the time constant t_b is also strongly dependent on fracture aperture, varying as b^2. Note that the "hydraulic" aperture used in the cubic law need not be equal to the parameter b in this report which is the "volumetric" aperture. In practice, on may take the hydraulic aperture to be smaller than the volumetric aperture.

A detailed examination of the first order asymptotic approximations of the fracture penetration h in column 3 of Table II reveals a strictly monotonic relationship between h and the parameters K_f, t_b, and t_a throughout the various flow periods. During all flow periods h varies linearly with K_f. With respect to the time constants t_b and t_a, the fracture penetration h varies as $t_b^{1/2}$ during flow period II and as $(t_b/t_a)^{1/2}$ during period III if $(t_b/t_a)^{1/2} << 1$. Based on reasonable estimates of K_f, t_b, and t_a, it is possible to obtain an upper bound approximation of h throughout flow periods I and II. For later flow periods, the asymptotic approximations of h are not conservative, in the sense of being an upper bound to fracture penetration, but are seen to compare reasonably well with the numerical solutions. In performing calculations that are to be conservative with respect to fracture penetration depth, one should therefore overestimate t_b and underestimate t_a. Comparisons with numerical solutions suggest that the asymptotic approximation is generally a strict upper bound for $t < t_{a1}$ and a reasonably close approximation to the solution for $t > t_{a1}$. Of course, these conclusions rely on the assumptions in our theory.

The dependence of the fracture penetration on t_b and t_a has a firm physical interpretation. Increasing t_b or decreasing t_a corresponds to decreasing the matrix imbibition flux. Hence, a greater fraction of the liquid remains in and continues to flow down the fracture, resulting in an increase in the fracture penetration rate. This physical reasoning applies even for situations with spatial variations in matrix properties.

An upper bound to the fracture penetration h can be estimated by choosing conservative values of t_a and t_b. This approach applies even for situations in which the matrix properties vary with respect to longitudinal position along the fracture. However, the asymptotic approximations were derived under the assumption that matrix properties do not spatially vary transverse to the fracture. Any spatial variations in matrix properties, such as reduced permeability in a region near the fracture, would require that a new imbibition function be derived, either analytically or numerically, which will conservatively

underbound the local imbibition flux for all longitudinal locations along the fracture. This new imbibition function would then be used to rederive the asymptotic approximations through the use of the techniques described in Nitao [1989].

9. Comparison with Numerical Solutions

In this section we give a brief overview of the comparison of the asymptotic solutions with those obtained numerically. The asymptotic expansions were compared with two separate types of numerical solutions. The first approach involved comparison of the asymptotic solutions with numerical solutions of the integro-differential equation (3.11). The method of solution is given in Nitao [1989]. The first-order asymptotic solutions along with the numerical solution are given in Figure 14 for the case of gravity-driven flow with the fracture entrance kept at ambient pressure. Note that the asymptotic solutions adequately capture the behavior of the solution and except for late times, appear to be conservative upper bounds to the fracture penetration by the liquid front.

The integro-differential equation upon which the analytical theory is based was derived under the assumption that the flow in the matrix is orthogonal to the fracture. In actual fracture systems this assumption may not be exactly satisfied. Moreover, under certain conditions, the flow in the fracture may be better represented as that in a porous medium rather than a front, as we have assumed. It is desirable then to compare our solutions with a two-dimensional simulation not containing these a priori assumptions. Therefore, the second numerical approach used in our comparison involves the two-dimensional simulation of fracture/matrix flow using a modified version of the TOUGH integrated finite difference code [Preuss and Wang, 1985; Nitao, 1988]. The code simultaneously solves three balance (continuum) equations for three components: air mass, water mass, and energy. (Although the energy balance was solved in our simulations, it is extraneous since our simulations were under isothermal conditions.)

The properties of the fracture used in the two-dimensional simulation are the same as those used by Buscheck and Nitao [1988a]. The model represents one out of an infinite set of fractures that are vertical and uniformly spaced. By symmetry, we need only model half the fracture and the matrix that is on one side; a lateral no-flow boundary is placed down the center of the fracture, and another down the center of the matrix block to represent the symmetry line with the neighboring fracture. The fracture is represented by a vertical column of grid blocks with porous media properties considered to be

characteristic of variably saturated flow in a fracture with a nominal aperture of 100 μm. The absolute permeability of the fracture is based on the "cubic law" for flow between parallel plates as given by Pouiselle flow theory. The fracture relative permeability curve is estimated by Wang and Narasimhan [1985] based on a simple conceptual model of fracture flow. The suction pressure versus saturation curve for the fracture was extrapolated, using the Young-Laplace equation [Adamson, 1982], from a curve which Wang and Narasimhan [1985] estimated on the basis of a simple conceptual model of fracture flow. One run was made with this suction curve while another run was made with suction set identically to zero in the fracture to see the effect of fracture capillary. In order to facilitate the interference between neighboring fractures to occur early in time a small fracture half-spacing of a = 2.26 cm is assumed.

As in Buscheck and Nitao [1988a], the matrix properties, including the characteristic curves which are non-linear, are based on measurements made by Peters and others [1984] on sample G4-6 (a sample of Topopah Spring densely welded tuff cored at a depth of 1158 feet within the repository interval at Yucca Mountain). The matrix porosity and initial saturation are taken to be 20 and 65 percent, respectively.

Table VIII is a summary of the fracture and matrix properties used in the two-dimensional model. The first six properties apply to the two-dimensional model. The last two, σ and t_b, are parameters required in the comparison with the asymptotic approximation. Recall that t_b is the approximate time at which the cumulative matrix imbibition flux is comparable to the specific fracture volume. For early times $t << t_a$, it can be shown [Nitao, 1989] that the first-order asymptotic approximation of the instantaneous specific volumetric imbibition flux, q, is given in terms of t_b and b by

$$q \sim \frac{b}{\sqrt{t\, t_b}} \tag{9.1}$$

Integrating (9.1) with respect to time, we get the cumulative imbibition flux, Q_m:

$$Q_m \sim 2b\sqrt{t/t_b} \tag{9.2}$$

By setting $t = t_b$ in (9.2), we get:

$$Q_m \sim 2b \tag{9.3}$$

One practical way of determining t_b is as follows. From a one-dimensional matrix imbibition model (where the upstream boundary condition is maintained at 100 percent saturation), the imbibition penetration depth of the saturation front into the matrix, d_{imb} is plotted against time. The front position

can be taken to be the point where the saturation is equal to the average of the maximum and initial saturations. The time that corresponds to $d_{imb} = 2b/(\phi(1-S_i))$ is equal to t_b. The effective matrix diffusivity, σ, is obtained by applying this value of t_b to equation (4.5). We applied this procedure to our example using the plot of log d_{imb} versus log t found in Buscheck and Nitao [1988a]. Another method would be to plot the cumulative imbibition flux. The time at which the flux equals $2b/(\phi(1-S_i))$ is t_b.

In comparing the plots of log $\bar{h}$ versus log τ obtained from the first-order asymptotic approximation and the two-dimensional numerical model (Figure 15), we find the two methods agreeing reasonably well. The figure shows two numerical solutions, one with fracture capillary, the other without. The asymptotic solutions given for these two cases are different only for early times $t << \bar{p}_0$ when fracture capillarity dominates. Since the two-dimensional numerical model models the fracture flow characteristics as a porous medium with a saturation-dependent capillary suction curve, it is not immediately obvious which value of capillary pressure drop p_c to use in the expression for the non-dimensional pressure drop term $\bar{p}_0$ $(= p_c / K_f t_b)$ needed in the asymptotic expansions. In column 4 of Table II we see that the lowest-order contribution of the suction during flow period II is a constant term $2\bar{p}_0/(\pi-2)$ so that the difference between a simulation with and without fracture capillarity will enable us to solve for this quantity. This fact was confirmed in our simulations. The value we obtained from this procedure, $\bar{p}_0 \simeq 0.3$, was used in obtaining the asymptotic expansion for $\tau \leq \bar{p}_0$ shown in Figure 15.

During flow period II ($\tau_b \leq \tau \leq \tau_b$), the asymptotic approximations and the two-dimensional model both result in a slope of $m = 0.5$. The small reduction in fracture penetration predicted by the two-dimensional model relative to the asymptotic solution is primarily the result of relative permeability effects in the fracture. It appears on the logarithmic plot as an almost constant downward shift in the two-dimensional model curve. Recall that while the asymptotic solution assumes front flow in the fracture, the two-dimensional model utilizes a relative permeability curve for fracture flow. The 26 percent reduction in fracture penetration corresponds to a fracture relative permeability, $k_r = 0.74$. Based on the fracture relative permeability curve, $k_r = 0.74$ corresponds to a fracture saturation of 95 percent. We found that for much of the wetted interval during flow period II, the fracture saturation is close to 95 percent. During flow period III ($\tau_a < \tau$), the two methods agree very well, with both methods yielding a slope of $m = 1$. Because for much of wetted interval of the matrix is fully saturated, capillary equilibrium between the matrix and fracture (in the two-dimensional model) results in the fracture being fully saturated (corresponding to $k_r = 1$). Consequently, saturation conditions in the fracture (in the two-dimensional model) result in front flow and there is no reduction in fracture penetration (relative to

the asymptotic solution) as was observed during flow period II.

This numerical simulation with its two-dimensional description of matrix flow with gravity and saturation dependent diffusivity function serves to confirm the validity of our basic assumptions underlying our simplified governing equations. Percentage deviation between numerical and approximate analytical solutions is greatest in the transition between flow period I and II and is about 50 percent. Although using higher-order terms may decrease this figure somewhat, we recall from the previous section that the problem is highly sensitive to various parameters such as the fracture aperture that are difficult to measure and are found to have high variability in the field. Thus, we feel that for most applications it is inappropriate and of dubious value to seek more complex solutions of higher accuracy.

Table VIII. Fracture and Matrix Properties Used in the Two-Dimensional Fracture/Matrix Model

b	45 μm
a	2.26 cm
K_f	8.17×10^{-3} m/s
K_m	1.86×10^{-11} m/s
ϕ	20 percent
S_i	65 percent
t_b	41.9 s
σ	3.10×10^{-8} m^2/s

10. Conclusions

We have analyzed various physical processes involved during one-dimensional fracture-dominated flow conditions in an unsaturated porous medium. Such a hydrological condition corresponds most likely to relatively high fluxes such as under ponding conditions at the fracture entrance. For various constant boundary conditions, approximate solutions to the movement of the liquid fracture front were derived. They show that the flow undergoes three major time periods characterized by physically interpretable time constants. The first time constant t_b is the time required for the matrix to imbibe a volume equal to that of the fracture storativity. The second is the time t_a for the imbibition front to reach the no-flow symmetry line of the neighboring fracture. The first time period occurs when $t << t_b$, the second when $t_b << t << t_a$, and the third for $t_a << t$. Transition periods occur between these main periods. The flow in the matrix can be divided into zones corresponding to the

three major flow periods. In many cases it can be shown that, for sufficiently large time, the front in the matrix lags behind the fracture front at a fixed distance. Asymptotic solutions were given which show that the approximate quantitative behavior of the liquid front can be conveniently represented by line segments when plotted on a log-log scale. The solutions can be used to understand the dependence on various physical parameters. We noted that in the case of constant boundary pressure head at the fracture entrance, the flux into a downward-inclined fracture under the influence of gravity was shown to be nearly constant in value. Thus, the fracture, in this case, acts to a certain extent as a flow rate regulating system. For a horizontal fracture the cumulative infiltration rate was shown to have an intermediate period during which it has a $t^{3/4}$ time dependence as opposed to the $t^{1/2}$ encountered in imbibition into a homogeneous medium. Therefore, a fractured medium cannot always be approximated by a single homogeneous porous medium. We also showed how the theory has implications to the drainage capacity of a fracture and to what flux conditions under which the liquid front of water in the fracture remains a continuous phase.

Comparison between the asymptotic and numerical solutions confirm the validity of the approach. Our solutions have the potential for estimating the front movement in many practical applications. In addition they present a better quantitative and qualitative understanding of the flow in a fracture in unsaturated porous media. These solutions may be helpful in the verification of numerical models of fracture flow.

There is still much work left to be done. Some of the areas which we hope to study are listed as follows.

1. determine the range of validity of the approximate analytical solutions
2. find what new effects are present in two-dimensional fracture flow
3. extend the analytical model, if possible, to fracture networks

In Part II, which is a companion paper [Nitao, 1989], we give the derivation of the asymptotic solutions presented in this first part. It includes, in some cases, closed form solutions, and the time dependent boundary value problem is also considered. Future work will present numerical simulations of fracture flow including interpretation of the results using the theory described in this paper. The transition point between fracture and matrix dominated flow will also be described in a future work. A report is also being planned to discuss the implications of our analysis including practical applications in the context of nuclear waste disposal at the proposed Yucca Mountain repository site.

References

Adamson, Arthur, W., *Physical Chemistry of Surfaces*, John Wiley and Sons, 4th ed., p. 8 (1982). NNA.891128.0580

Beven, K. and Germann, P., Macropores and Water Flow in Soils, *Water Resources Research*, vol. 18, no. 5, 1311-1325 (1982). NNA.890327.0050

Bokserman, A.A., Zheltov, Yu. P., and Kocheshkov, A.A., Motion of Immiscible Liquids in a Cracked Porous Medium, *Soviet Physics-Doklady*, vol. 9, no. 4 285-287 (1964). NNA.89110° 0051

Buscheck, T.A. and Nitao, J.J., *Estimates of the Impact of Drilling Water on the Near Field Hydrology for In Situ Experiments in Densely Welded Tuff*, Lawrence Livermore National Laboratory, UCID-21294 (1988a). NNI.881219.0030

Buscheck, T.A. and Nitao, J.J., *Estimates of the Width of the Wetting Zone Along a Fracture Subjected to an Episodic Infiltration Event in Variably Saturated, Densely Welded Tuff*, Lawrence Livermore National Laboratory UCID report, in preparation (1988b). NNA.891109.0065

Davidson, M. R., Asymptotic Infiltration into a Soil which Contains Cracks or Holes but whose Surface is Otherwise Impermeable, *Transport in Porous Media*, vol. 2, 165-176 (1987). NNA.891109.0052

Klavetter, E.A., and Peters, R.R., *Fluid Flow in a Fractured Rock Mass*, Sandia National Laboratories, SAND85-0855 (1986). NNA.870721.0004

Marle, C.M., *Multiphase Flow in Porous Media*, Gulf Pub. Co., p. 141-143, (1981). NNA.891109.0040

Martinez, M.J., *Capillary-Driven Flow in a Fracture Located in a Porous Medium*, Sandia National Laboratories, SAND84-1697 (1988). NNI.880928.0024

Montazer, P. and Wilson, W.E., *Conceptual Hydrologic Model of Flow in the Unsaturated Zone, Yucca Mountain, Nevada*, U.S. Geological Survey, Water-Resources Investigations Report 84-4345 (1984). NNA.870519.0109

Nitao, J.J., *Numerical Modelling of the Thermal and Hydrological Environment around Nuclear Waste Package Using the Equivalent Continuum Approximation: Horizontal Emplacement*, Lawrence Livermore National Laboratory report UCID-21444 (1988). NNI.880630.0013

Nitao, J.J., *On the Movement of a Liquid Front in an Unsaturated, Fractured Porous Medium, Part II. --- Mathematical Theory*, Lawrence Livermore National Laboratory UCID report, (1989). NNA.891130.0051

Peters, R.R., Klavetter, E.A., Hall, I.J., Blair, S.C., Heller, P.R., and Gee, G.W., *Fracture and Matrix Hydrologic Characteristics of Tuffaceous Materials from Yucca Mountain, Nye County, Nevada*, Sandia National Laboratories report no. SAND84-1471 (1984). NNA.870407.0036

Philip, J.R., The Theory of Absorption in Aggregated Media, *Australian Journal of Soil Research*, vol. 6, 1-19 (1968). NNA.891128.0581

Pruess, K. and Wang, J.S.Y., TOUGH - A Numerical Model for Nonisothermal Unsaturated Flow to Study Waste Cannister Heating Effects, *Mat. Res. Soc. Symp. Proc.*, vol. 26, Elsevier Science (1984). NNA.891109.0043

Travis, B.J., Hodson, S.W., Nuttall, H.E., Cook, T.L., and Rundberg, R.S., *Preliminary Estimates of Water Flow and Radionuclide Transport in Yucca Mountain, Los Alamos National Laboratory*, LA-UR-84-40 (1984). HOS.880517.1909

van Golf-Racht, T.D., *Fundamentals of Fractured Reservoir Engineering*, Elsevier (1982). HQZ.870227.3605

Wang, J.S.Y. and Narasimhan, T.N., Hydrologic Mechanisms Governing Fluid Flow in a Partially Saturated, Fractured, Porous Medium, *Water Resources Research*, vol. 21, no. 12, 1861-1874 (1985). NNA.891109.0050

Witherspoon, P.A., J.S.Y. Wang, K. Iwai, and J.E. Gale, Validity of the Cubic Law for Fluid Flow in a Deformable Rock Fracture, *Water Resources Research*, vol. 16, no. 6, 1016-1024 (1980). NNA.891109.0039

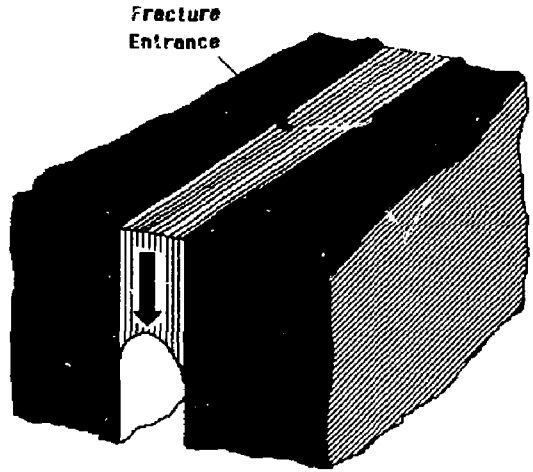

Figure 1. Idealized Fracture

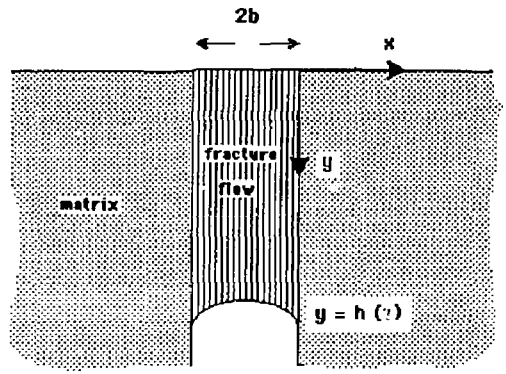

Figure 2. Fracture Coordinate System

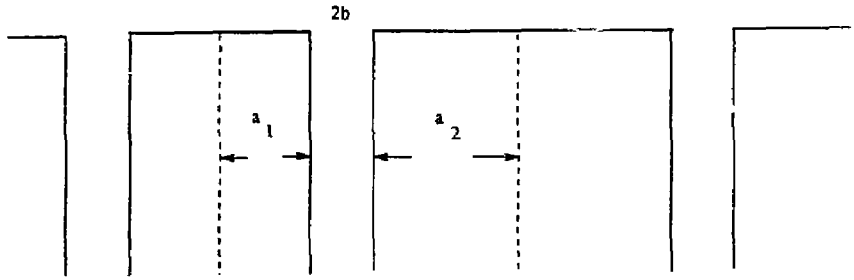

Figure 3. Geometry of Parallel Fracture System

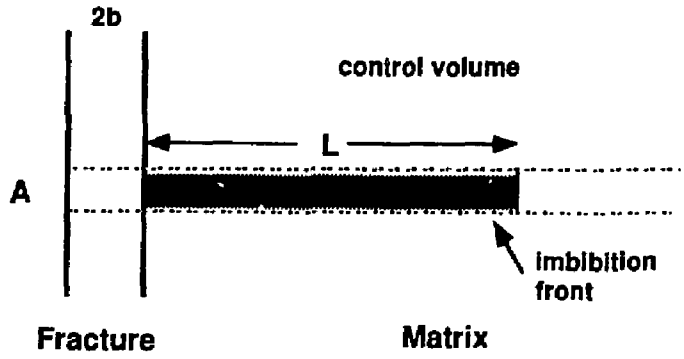

Figure 4. Control Volume for Matrix Imbibition

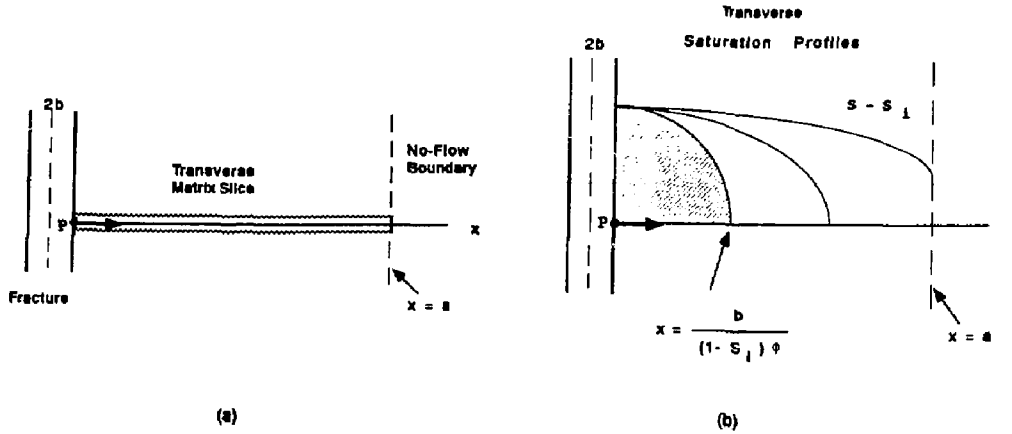

Figure 5. Stages in Matrix Imbibition

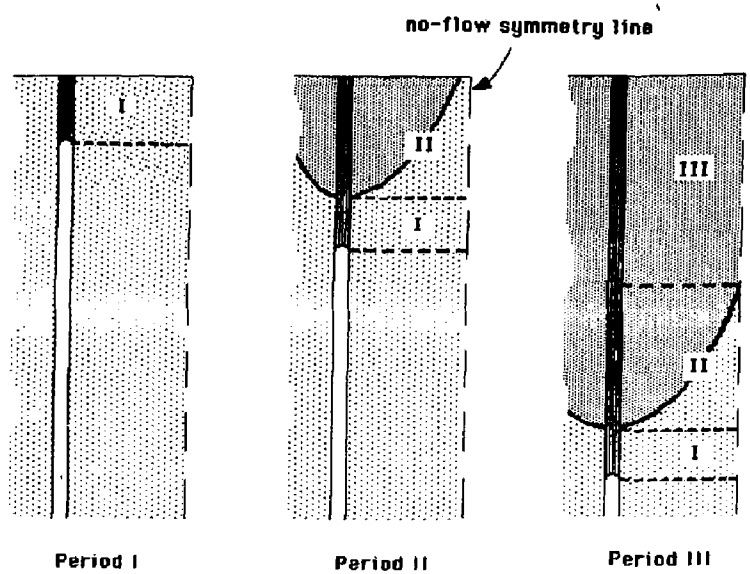

Figure 6. Flow Periods and Matrix Zones

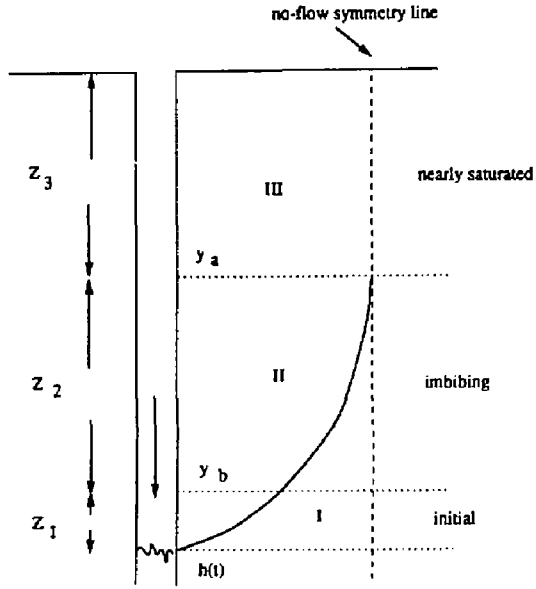

Figure 7. Matrix Zones

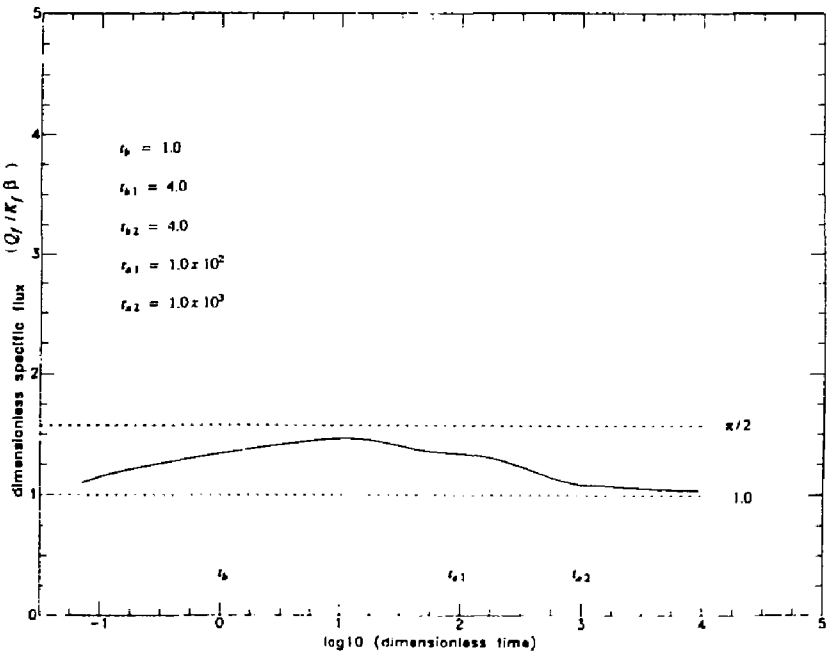

Figure 8. Specific Fracture Influx q_f for Gravity Driven Flow with $p_0 = 0$

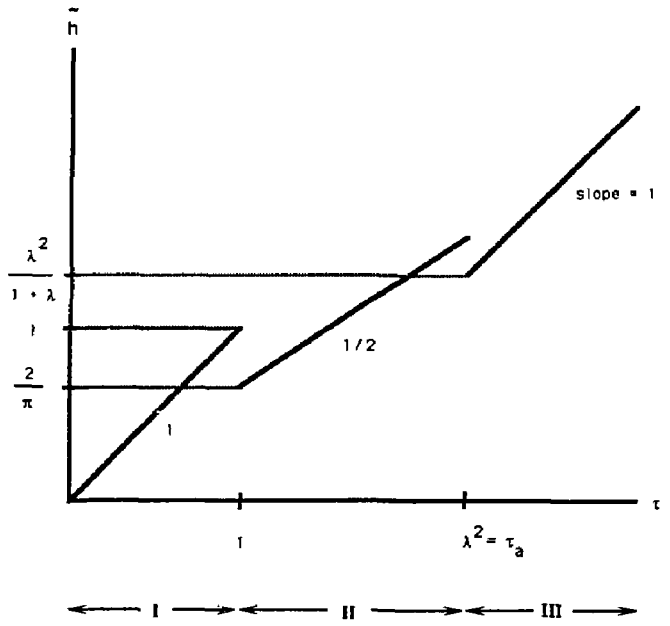

Figure 9. Asymptotic Profiles for Flux Boundary Condition (Log-Log)

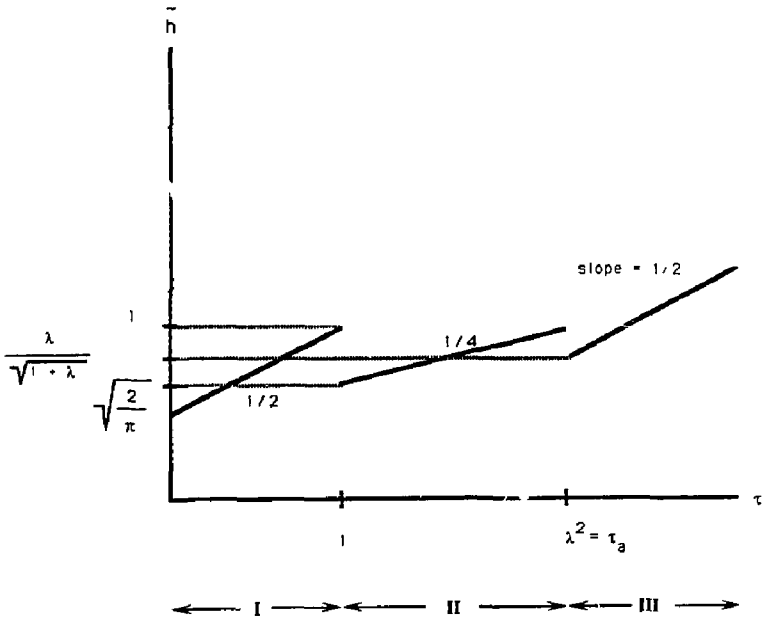

Figure 10. Asymptotic Profiles for Pressure Boundary Condition, No Gravity (Log-Log)

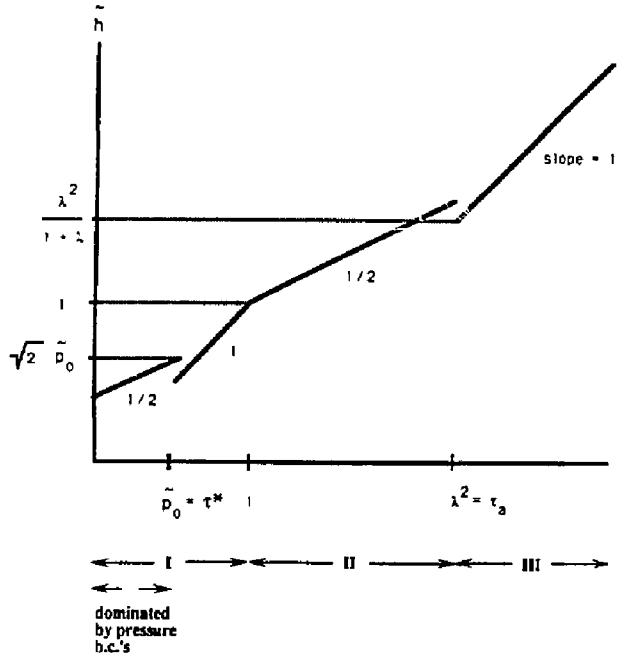

Figure 11. Asymptotic Profiles for Non-Zero Pressure Boundary Condition, $\tilde{p}_0 \leq 1$ (Log-Log)

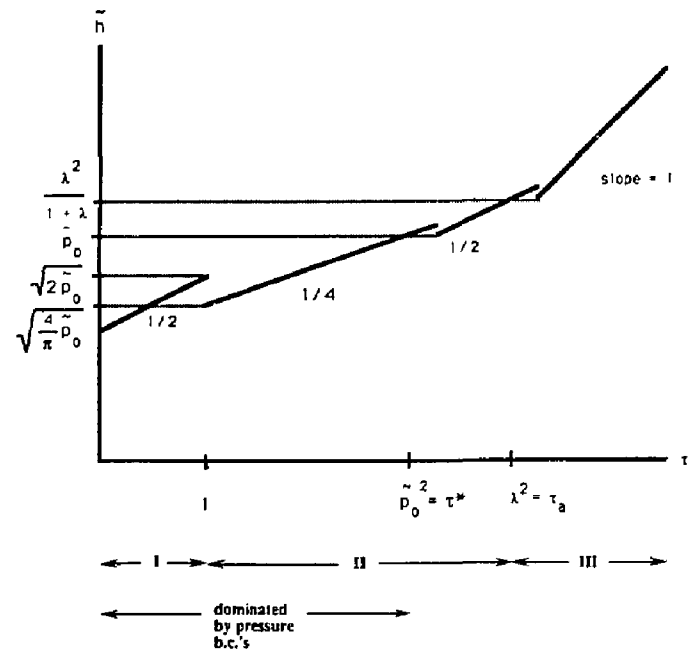

Figure 12. Asymptotic Profiles for Non-Zero Pressure Boundary Condition, $1 \leq \tilde{p}_0 \leq \lambda$ (Log-Log)

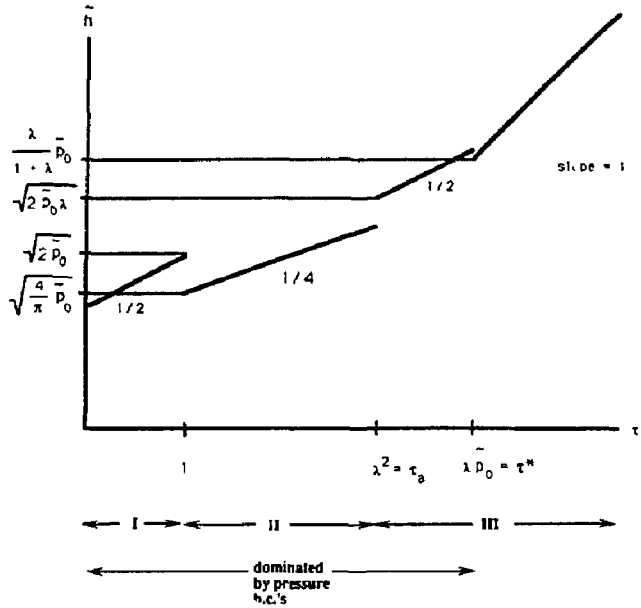

Figure 13. Asymptotic Profiles for Non-Zero Pressure Boundary Condition, $\lambda \leq p_0$ (Log-Log)

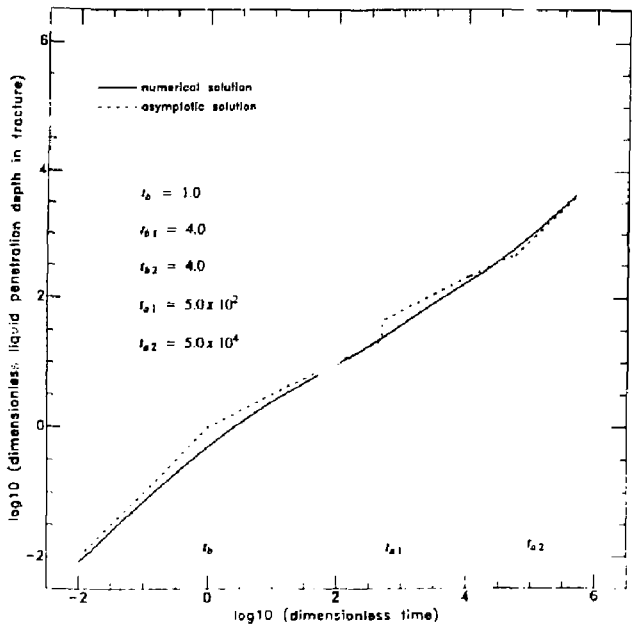

Figure 14. Comparison of First Order Asymptotic Solutions with Numerical Solution to Integro-Differential Equation (zero fracture capillarity, $a_1 << a_2$) (Log-Log)

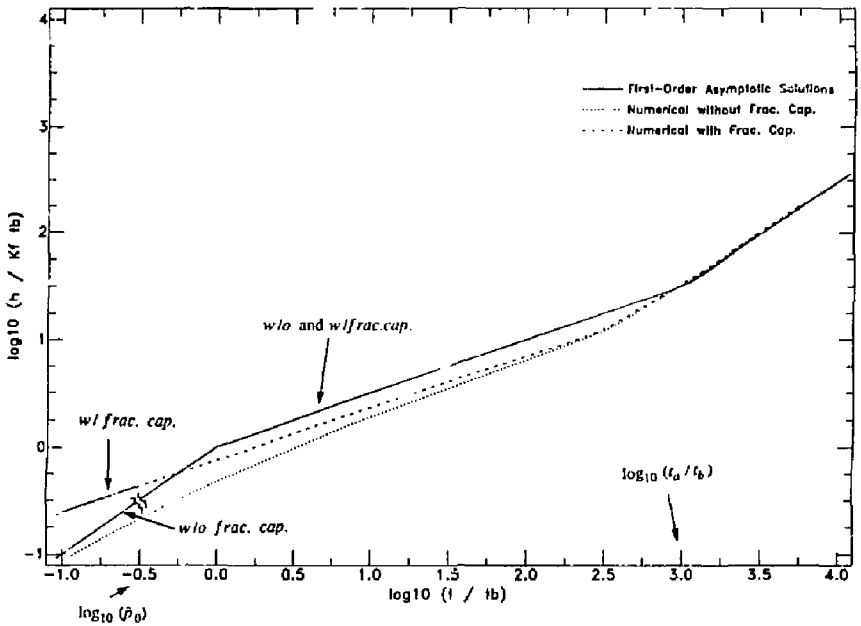

Figure 15. Comparison of First Order Asymptotic Solutions with Two-Dimensional Numerical Solution (non-zero fracture capillarity, $a_1 = a_2$) (Log-Log)

The following number is for Office of Civilian Radioactive Waste Management Records Management purposes only and should not be used when ordering this document:

Accession Number: NNA.891130.0050